ACS Macro Letters

pubs.acs.org/macroletters Letter

Visible-Light HAT Photocatalysis for Switchable Polyethylene Degradation and C−H Functionalization

Manish Kumar, Zhisheng Lin, Stephen Don Sarkar, Eva Harth,* and Cyrille Boyer*

Cite This: https://doi.org/10.1021/acsmacrolett.6c00309 Read Online

ACCESS | Metrics & More | Article Recommendations | Supporting Information

ABSTRACT: We report a hydrogen atom transfer (HAT)-mediated photocatalytic platform that switches between oxidative degradation and precision C−H functionalization of polyethylene (PE) by simple control of the reaction conditions. Under O_2, anthraquinone (AQ) catalyzes rapid chain scission under visible light at room temperature, resulting in ∼90% reduction in molecular weight (M_n) and oxidized compounds. In contrast, under anaerobic conditions, the reaction is redirected toward functionalization of PE, enabling grafting of maleimide and maleic anhydride onto the PE backbone without chain degradation. Grafting efficiency is tunable and verified by NMR, FTIR, and DOSY, while anhydride handles enable downstream derivatization to amide-functionalized materials.

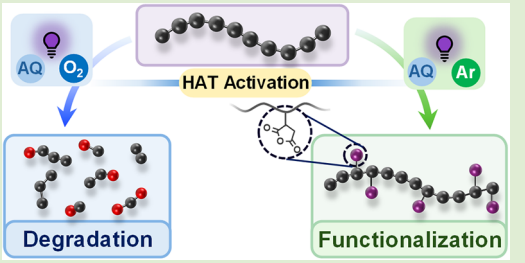

Since the emergence of large-scale plastic production in the 1950s, global output has expanded exponentially, exceeding 430 million tonnes in 2024 and projected to approach ∼670 million tonnes by 2040.[1,2] Among commodity plastics, polyethylene (PE) dominates (∼26% of total production; >100 million tonnes annually) owing to its low cost, chemical resistance, mechanical durability, and processability.[2−9] However, these same attributes, particularly its chemical inertness, underpin its environmental persistence, leading to long-term accumulation and associated ecological impacts.[10−13] Current recycling efforts remain inadequate to address the accelerating waste stream, with substantial fractions still landfilled, incinerated, or released into the environment.[10−12] These challenges highlight the urgent need for efficient strategies to valorize PE within a circular materials economy.

Polymer recycling strategies are broadly divided into mechanical and chemical approaches, both of which face intrinsic limitations. Mechanical recycling, while industrially established, suffers from cumulative chain scission and oxidative degradation, resulting in diminished material properties and microplastic formation.[14−17] In contrast, chemical recycling enables conversion into monomers, fuels, or value-added chemicals, offering a more flexible pathway toward circularity.[18−21] Despite notable progress in other polymers, such as upcycling of polystyrene (PS)[22−25] and efficient depolymerization of poly(methyl methacrylate) (PMMA) via thermal, photothermal, and electrochemical routes,[26−35] analogous strategies for PE remain underdeveloped. Existing methods, including heteroatom insertion, backbone oxidation, and catalytic cracking, are limited in scope and typically require harsh conditions, specialized infrastructure, or metal-based catalysts.[36−40] These constraints hinder scalability and increase environmental burden.

The fundamental barrier to PE upcycling lies in its chemically inert backbone, composed of strong C−C and C−H bonds and lacking functional handles.[41] Hydrogen atom transfer (HAT) chemistry has recently emerged as a powerful approach for activating strong C−H bonds under mild conditions.[42−45] Selective hydrogen abstraction generates carbon-centered radicals that can be directed toward either bond scission or functionalization.[46−50] This dual reactivity provides a conceptual framework to unify degradation and modification within a single mechanistic platform. Although HAT chemistry has demonstrated considerable potential in polymer contexts, including PMMA depolymerization,[51,52] PS upcycling,[22−25] and polymer chain and surface functionalization,[47,53] its use in PE transformation remains comparatively underdeveloped.[54−58] Recent approaches have enabled either oxidative degradation of polyolefins or direct backbone functionalization (e.g., thermal cracking, catalytic pyrolysis, oxidative degradation); however, these transformations are typically developed as separate processes and often require harsh conditions. This can lead to poorly controlled mixtures of products rather than allowing selective control over degradation versus functionalization pathways.[54−59]

Controlled degradation of PE into lower-molecular-weight oligomers is an attractive route to enhance processability and reactivity while mitigating environmental persistence.[60,61]

Received: June 4, 2026
Revised: July 6, 2026
Accepted: July 7, 2026

Scheme 1. General Route for Photocatalytic Degradation (Aerobic Condition) and Functionalization of PE (Anaerobic Condition) via HAT Chemistry

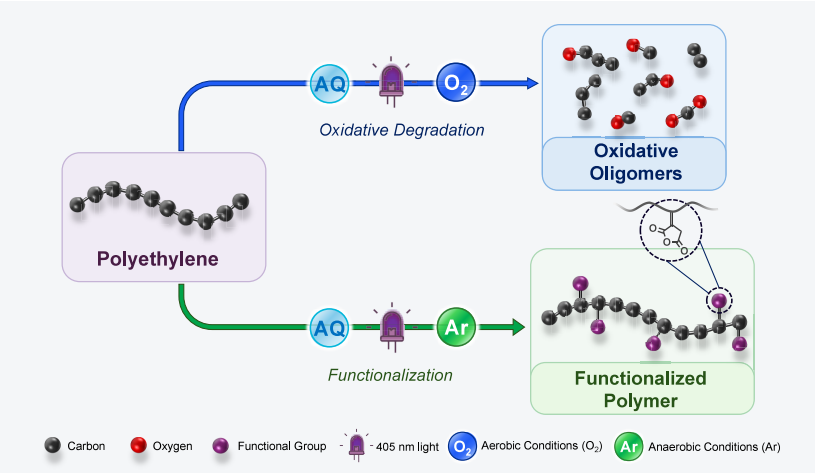

Complementarily, direct functionalization offers a route to increase material value. In particular, grafting maleic anhydride (MA) introduces polar functionality, improving adhesion, compatibility, and utility in blends, adhesives, and composites.[62,63] The anhydride moiety further enables downstream derivatization to acids, esters, and amides.[64] However, conventional MA grafting generally relies on high-temperature peroxide initiation, which can promote undesired chain scission, cross-linking, and poorly controlled graft structures.[65]

HAT-based photocatalysis provides a compelling alternative by enabling controlled radical generation directly from the PE backbone under mild conditions. Herein, we report a unified HAT-mediated strategy that enables divergent reactivity of polyethylene (Scheme 1). Using anthraquinone (AQ) as an organic photocatalyst, PE undergoes efficient oxidative chain scission in the presence of O_2, achieving up to ∼90% reduction in molecular weight (M_n) at room temperature. In contrast, under anaerobic conditions, the same HAT mechanism enables selective grafting of maleic anhydride and its derivatives. Mechanistic validation via a model substrate (e.g., dodecane) confirms efficient reactions, which translates directly to PE without concurrent degradation. Extension to maleimide (ME) and phenyl maleimide (PhME) introduces diverse functionality, while postfunctionalization of MA-grafted PE via amine coupling affords amide-functional materials. Collectively, the ability to switch between degradation and functionalization within a single HAT platform represents a significant advance in polymer upcycling. This work establishes a mild, metal-free, and mechanistically unified strategy for PE valorization, providing a foundation for sustainable plastic recycling and circular materials design.

Polyethylene (PE) degradation studies were initiated by dissolving the polymer in chloroform at a concentration of 5 g L^{-1} (178 mM in repeat units, [RU]). For this study, an amorphous, highly branched low-density PE with a branching density of 135/1000C was selected (SI, Schemes S1−S5 and Figures S1 and S2). Anthraquinone (AQ) was employed as a photocatalyst at a loading of 0.05 eq relative to [RU] ([RU]:[AQ] = 1:0.05). The solution was purged with oxygen and irradiated with 405 nm light (λ_{max} = 405 nm, 24 mW cm^{-2}) at 25 °C (Figure 1A and SI, Figure S3). Size exclusion chromatography (SEC) analysis revealed a pronounced shift in retention time toward lower molecular weights, indicative of efficient chain scission. After 24 h, the number-average molecular weight (M_n) decreased from 8900 g mol^{-1} to 1400 g mol^{-1} (∼84% reduction). Continued irradiation led to further degradation, reaching ∼800 g mol^{-1} (∼90% reduction) after 72 h (Figure 1C and Table S1). For a more quantitative assessment of the degradation efficiency, the area under the SEC traces was determined by normalizing the integration value (I) at 0 h to 100. This analysis showed that the polymer signal decreased to 47.1 and 37.6 after 24 and 72 h, respectively, corresponding to degradation efficiencies of 52.9% and 62.4% (SI, Figure S4 and Table S1). ^{1}H NMR analysis corroborated these findings, showing attenuation of characteristic PE backbone resonances (0.8−1.3 ppm) alongside the emergence of broad signals between 1.5−5 ppm and downfield features at 12−13 ppm, consistent with the formation of oxidative oligomeric species (Figure 1D). High-resolution mass spectrometry (HRMS) of the crude reaction mixture further confirmed the formation of low-molecular-weight oxidation products, including carboxylic acids (e.g., acetic, butanoic, and hexanoic acids) and glutaraldehyde (Figure 1B and SI, Figures S5−S8).

To substantiate the proposed oxidative degradation mechanism of polyethylene (PE), a model study was performed using dodecane as a surrogate substrate owing to its structural similarity to PE (SI, Scheme S6). When subjected to the same degradation conditions, ^{1}H NMR spectra exhibited resonances in the 9−13 ppm range consistent with aldehydic and acidic species. HRMS further identified a range of oxidized products, including carboxylic acids (butyric, hexanoic, and adipic acids) and dialdehydes (glutaraldehyde, heptanedial, and dodecanedial), corroborating a mechanism involving HAT followed by oxygen trapping and β-scission (SI, Figures S9−S15).

To further validate this oxidative degradation pathway and establish the necessity of each reaction component, a series of control experiments was performed. In the absence of light, photocatalyst, or oxygen, no measurable degradation was observed, as confirmed by unchanged SEC traces (SI, Figures S16−S18). These results highlight the need for the catalyst (AQ), light, and oxygen in promoting PE degradation. Building on this, we systematically investigated the influence of key reaction parameters on degradation kinetics.

https://doi.org/10.1021/acsmacrolett.6c00309
ACS Macro Lett. XXXX, XXX, XXX−XXX

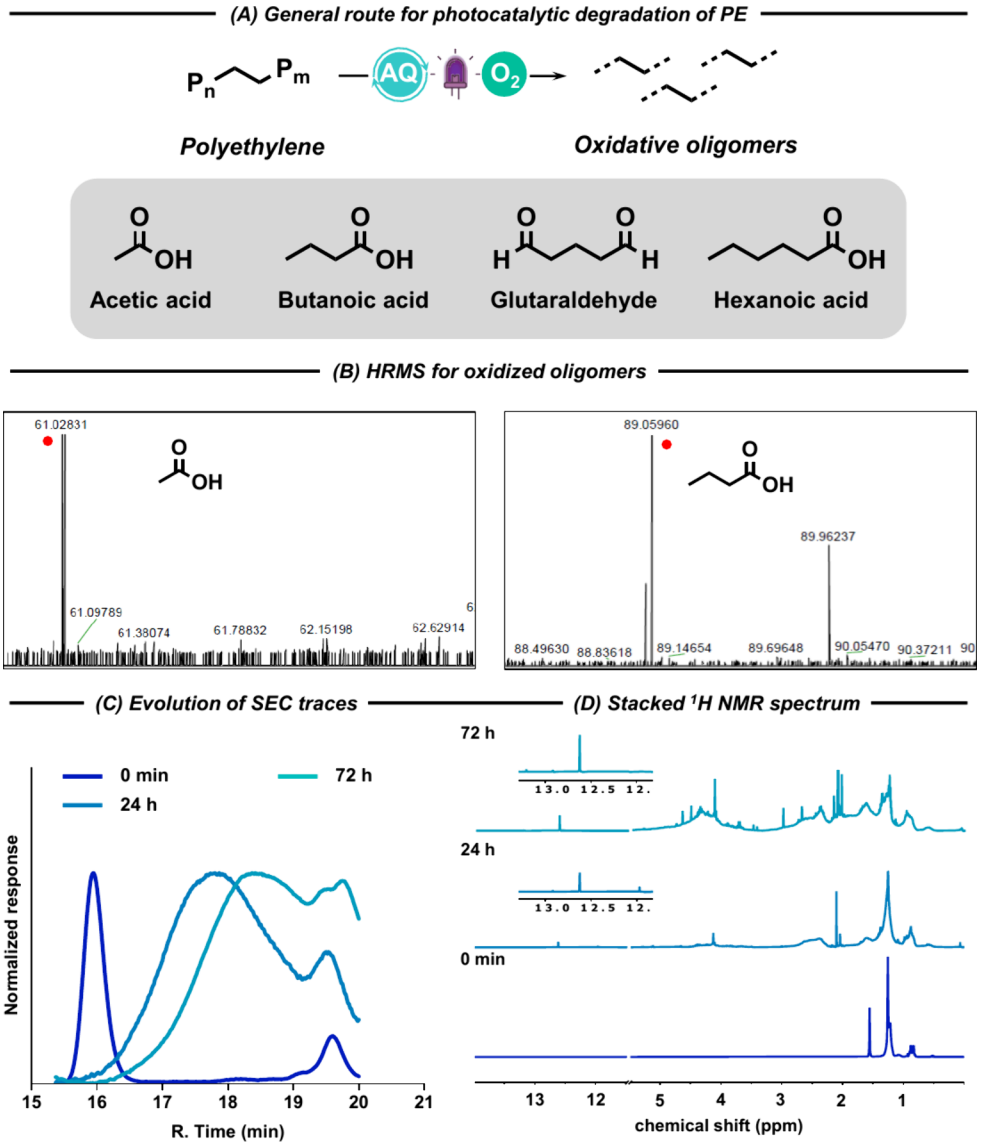

Figure 1. (A) General route for photocatalytic degradation of PE; (B) HRMS for the oxidized oligomers such as acetic acid (m/z 61.0283, calcd 61.0284) (left) and butanoic acid (m/z 89.0596, calcd 89.0597) (right); (C) Evolution of SEC traces with time for degradation of PE; (D) ^{1}H NMR spectra of the crude mixture at different time points showing degradation of PE. Reaction conditions: [RU] = 178 mM, [RU]:[AQ] = 1:0.05, temperature = 25 °C, atmosphere = O_2, λ_{max} = 405 nm, 24 mW cm^{-2}.

Given the central role of AQ in mediating hydrogen atom transfer (HAT), its concentration was varied relative to [RU]. Increasing catalyst loading led to a clear enhancement in degradation efficiency: at 0.0125 eq AQ, ∼70% reduction in M_n was observed after 24 h, increasing to ∼78% at 0.025 eq, and ∼84% at 0.05 eq (SI, Figure S19 and Table S2). This trend confirms a direct dependence of degradation kinetics on catalyst loading: higher AQ concentrations increase the flux of carbon-centered radicals generated by hydrogen abstraction from the PE backbone, thereby accelerating β-scission and chain fragmentation.

Temperature effects were also examined by irradiating PE solutions (5 g L^{-1}) containing 0.025 eq AQ at 40 and 60 °C. Surprisingly, higher temperatures led to diminished degradation efficiency. After 8 h, a 61% reduction in M_n was observed at 40 °C, compared to only 40% at 60 °C. Extending the reaction time to 16 h resulted in 86% degradation at 40 °C but only 57% at 60 °C (SI, Figure S20 and Table S3). To rationalize this unexpected behavior, ^{1}H NMR spectra of the reaction mixtures were analyzed. In addition to the reduction of PE backbone signals, a significant decrease in AQ aromatic signals (7.8−8.5 ppm) was observed at elevated temperatures, suggesting catalyst decomposition (SI, Figure S21). To further probe this, AQ degradation was studied independently under identical photochemical conditions. Solutions of AQ in chloroform were irradiated at 25, 40, and 60 °C, and monitored by UV−vis spectroscopy (λ = 327 nm). Minimal degradation (∼9% absorbance loss) was observed after 2 h at 25 °C, whereas 21% and 47% decreases were recorded at 40 and 60 °C, respectively (SI, Figure S22). These results indicate that elevated temperatures accelerate photothermal decomposition of AQ, reducing its effective concentration and impairing HAT activity. This accounts for the counterintuitive decrease in PE degradation efficiency at higher temperatures. Moderate heating (40 °C) nevertheless improves overall kinetics relative to 25 °C, achieving comparable degradation in shorter times (86% in 16 h vs 84% in 24 h). Collectively, these findings reveal a nuanced interplay among catalyst

https://doi.org/10.1021/acsmacrolett.6c00309
ACS Macro Lett. XXXX, XXX, XXX−XXX

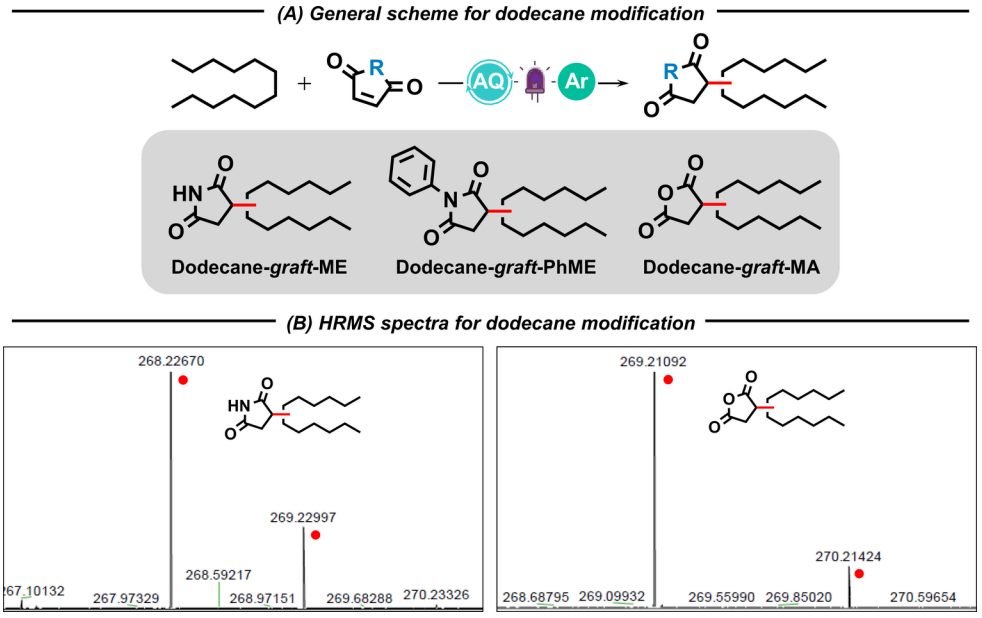

Figure 2. (A) General synthetic route for the dodecane modification; (B) HRMS spectrum of dodecane-*graft*-ME (m/z 268.2267, calcd 268.2271) (left) and dodecane-*graft*-MA (m/z 269.2109, calcd 269.2111) (right). Note: The second peaks at 269.2299 (left) (calcd 269.2305) and 270.2142 (right) (calcd 270.2145) observed in HRMS are attributed to the natural isotopic peaks (^{13}C) of the molecular ions.

stability, temperature, and reaction time, underscoring the importance of parameter optimization for efficient degradation.

Because the solubility of PE in chloroform limits the achievable polymer concentration, we next investigated whether the HAT degradation strategy remains effective at higher loadings using tetrachloroethane (TCE) as the solvent. With the [RU]:[AQ] ratio held constant at 1:0.05, raising the PE concentration from the standard 5 g L^{-1} (in chloroform) to 20 g L^{-1} reduced the SEC-determined degradation efficiency from 52.9% to 36.9% after 24 h, and a further increase to 50 g L^{-1} lowered it to 17.0% (SI, Figure S23 and Table S4). Thus, although efficiency decreased monotonically with increasing concentration, appreciable chain scission was retained even at a 10-fold higher loading. This persistent activity at substantially higher polymer concentrations highlights the robustness of the HAT platform and its potential to operate under more process-relevant conditions. Overall, this HAT-based approach enables effective PE degradation under mild conditions, offering a compelling, metal-free alternative to conventional high-temperature pyrolysis.

After degradation, we next turned our attention to the functionalization of PE without inducing chain scission. Leveraging the same HAT strategy, carbon-centered radicals generated on the polymer backbone were reacted with suitable radical acceptors (Figure 2A and SI, Figure S24). Prior to polymer modification, dodecane was again used as a model substrate to evaluate grafting reactions, which were carried out under argon to suppress oxidative side reactions. Dodecane was reacted with maleimide (ME) in the presence of AQ under 405 nm irradiation (λ_{max} = 405 nm, 24 mW cm^{-2}) (SI, Scheme S7). The crude product was analyzed by ^{1}H NMR and high-resolution mass spectrometry (HRMS), confirming formation of dodecane-*graft*-ME (m/z 268.2267, calcd 268.2271) (Figure 2B and SI, Figures S25 and S26). Notably, signals corresponding to multiple grafted products were also observed (m/z 365.2430, calcd 365.2434) (SI, Figure S25). Analogous reactions with phenyl maleimide (PhME) afforded dodecane-*graft*-PhME, again showing both mono- and difunctionalized products (m/z 344.2582 and 517.3058, respectively) (SI, Scheme S8 and Figures S27 and S28). Similarly, maleic anhydride (MA) was successfully grafted, yielding dodecane-*graft*-MA (m/z 269.2109, calcd 269.2111) (SI, Scheme S9 and Figures S29 and S30). These model studies demonstrate that HAT-mediated radical generation enables functionalization of otherwise inert aliphatic C−H bonds.

Encouraged by these results, the methodology was extended to PE. Functionalization of PE is inherently challenging given its chemically inert, hydrophobic backbone, yet introduction of polar groups via grafting offers a direct route to modulate material properties. PE (5 g L^{-1}, 178 mM [RU]) was dissolved in chloroform, followed by the addition of ME and AQ. The mixture was irradiated after purging with argon to suppress oxidative degradation (SI, Scheme S10). The resulting PE-*graft*-ME was purified by repeated precipitation in cold methanol. SEC analysis confirmed that no significant chain scission occurred during functionalization (SI, Figure S31). Next, FTIR spectroscopy showed characteristic carbonyl (C═O) stretching bands (~1530−1870 cm^{-1}), confirming successful grafting (SI, Figure S32). ^{1}H NMR further supported this, with new resonances appearing between 2.4−3.2 ppm (SI, Figure S33). To increase grafting density, ME loading was varied from 10% to 30% relative to the PE repeat unit ([RU]). For comparison, the polyethylene backbone signal (2670−3020 cm^{-1}) was normalized to 100 in FTIR analysis, revealing an increase in relative carbonyl intensity in the 1530−1870 cm^{-1} region (Table S5). While FTIR integration is semiquantitative, the systematic increase in carbonyl intensity with ME loading clearly reflects enhanced graft incorporation.

To obtain more quantitative insight, PhME was employed (SI, Scheme S11). The grafting and purification procedures were carried out under analogous conditions. FTIR analysis of PE-*graft*-PhME showed characteristic carbonyl (C═O) stretching bands in the 1530−1870 cm^{-1} region, consistent

https://doi.org/10.1021/acsmacrolett.6c00309
ACS Macro Lett. XXXX, XXX, XXX−XXX

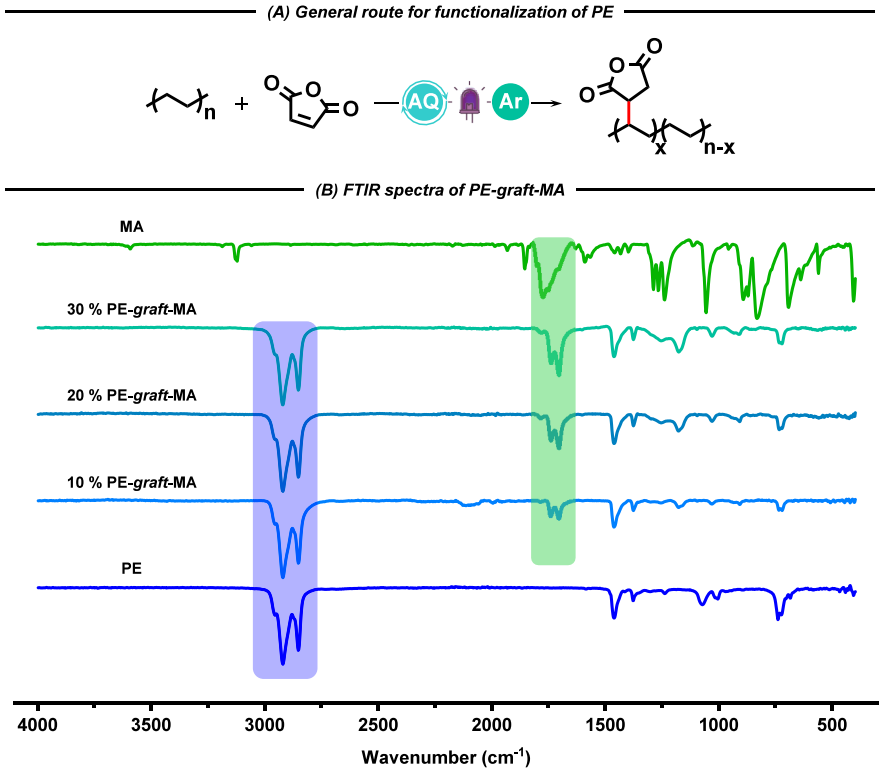

Figure 3. (A) General synthetic route for the preparation of PE-*graft*-MA; (B) IR spectra of PE-*graft*-MA synthesized with an added MA amount of 10, 20, and 30 mol % of PE repeat unit [RU] where the green-shaded region (1530−1870 cm^{-1}) corresponds to the carbonyl (C═O) groups of MA, and the blue-shaded region (2670−3020 cm^{-1}) corresponds to the alkane (C−H) bonds of PE.

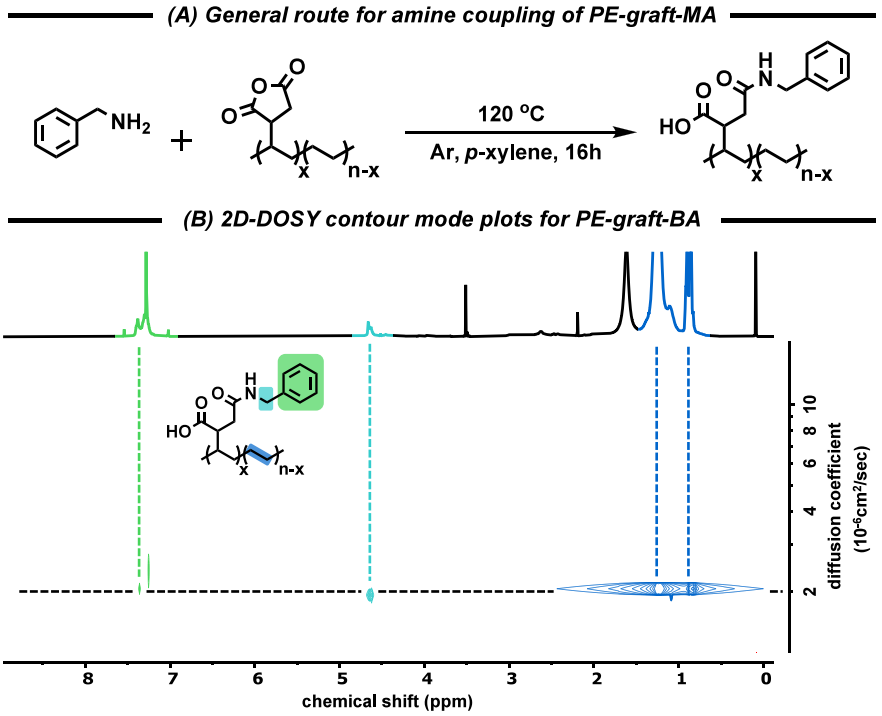

Figure 4. (A) General synthetic route for the amine coupling of PE-*graft*-MA using benzylamine; (B) 2D-DOSY contour mode plots for PE-*graft*-BA recorded in $CDCl_3$.

with successful incorporation of PhME units (SI, Figure S34). The integrated intensity of this band increased from 9.6 to 24.8 upon increasing PhME loading from 10% to 20% relative to the PE repeat unit ([RU]) (Table S6). To further quantify grafting, ^{1}H NMR spectroscopy was employed (SI, Figure S35). For the 20% PhME-functionalized sample, the aromatic proton signal at ∼7.4 ppm was integrated relative to the PE backbone methylene resonance at ∼1.2 ppm, yielding a

https://doi.org/10.1021/acsmacrolett.6c00309
ACS Macro Lett. XXXX, XXX, XXX−XXX

grafting yield of 8.82%, corresponding to approximately 5.6 PhME units per PE chain (SI, eq 1). Two-dimensional diffusion-ordered spectroscopy (2D DOSY) NMR further confirmed successful covalent attachment. The stacked DOSY spectra showed that the signals at 1.2 ppm (PE backbone) and 7.4 ppm (PhME aromatic protons) exhibit identical attenuation behavior (SI, Figure S36). Consistently, DOSY contour analysis revealed a shared diffusion coefficient in the order of 10^{-6} cm^2 s^{-1} for both resonances, indicating that they originate from the same molecular species (SI, Figure S37). The absence of olefinic PhME signals (~6.8 ppm) further confirms complete incorporation. Together, these data provide unambiguous evidence for covalent grafting of PhME onto the PE backbone.

Following the successful modification of PE with ME and PhME, we extended the strategy to maleic anhydride (MA), a widely used grafting monomer in industrial polyolefin modification.[65] PE-*graft*-MA was synthesized under analogous conditions and characterized by SEC and ^{1}H NMR, which revealed new resonances between 2.2 and 4.4 ppm (Figure 3A and SI, Figures S38 and S39). FTIR spectroscopy further confirmed successful grafting through the appearance of carbonyl (C═O) stretching bands in the 1530−1870 cm^{-1} region, consistent with anhydride functionality (Figure 3B). PE-*graft*-MA samples were prepared with three different MA feed ratios (10, 20, and 30%), yielding PE-*graft*-MA materials (Table S7). Increasing MA feed ratios (10−30%) led to corresponding increases in integral values of carbonyl signal intensity (11.6 (10%) to 20.8 (20%) and 43.0 (30%)), confirming tunable grafting density.

Beyond its industrial relevance, MA grafting provides a versatile platform for further derivatization, as the anhydride moiety can be readily transformed into acids, esters, and amides. As a demonstration, PE-*graft*-MA was subjected to amine coupling with benzylamine in *p*-xylene at 120 °C under argon (Figure 4A). The resulting PE-*graft*-BA was purified by precipitation in cold methanol to remove unreacted amine. ^{1}H NMR analysis showed a downfield shift of the benzylic CH_2 resonance from 3.8 to 4.6 ppm upon amide formation (SI, Figure S40). Aromatic signals at ~7.3 ppm were also observed and used to estimate a grafting density of 10.9 amide groups per PE chain. FTIR further confirmed successful conversion, where the initial broad and bimodal C═O band (1530−1870 cm^{-1}) became sharper and monomodal after amine coupling in PE-*graft*-BA (SI, Figure S42). DOSY experiments again confirmed covalent attachment, with all relevant signals, including the PE backbone (1.3 ppm), benzylic CH_2 (4.6 ppm), and aromatic protons (7.3 ppm), showing identical diffusion coefficients (Figure 4B and SI, Figure S41).

To further demonstrate the versatility of this postfunctionalization strategy, an aliphatic hexylamine was employed as an alternative nucleophile. Under analogous conditions, PE-*graft*-HA was obtained and similarly characterized by ^{1}H NMR and FTIR (SI, Scheme S12 and Figures S42 and S43). Consistent with benzylamine coupling, characteristic spectral shifts were observed in ^{1}H NMR, while again FTIR showed conversion of the anhydride band from a broad bimodal feature in PE-*graft*-MA to a sharper monomodal carbonyl profile in PE-*graft*-HA, confirming successful amide formation.

In summary, we have established a unified HAT-mediated photocatalytic platform for switchable PE valorization, toggling between oxidative degradation and precision C−H functionalization within a single mechanistic framework. Under aerobic conditions, AQ-mediated hydrogen atom transfer promotes efficient oxidative chain scission, delivering up to ~90% reduction in molecular weight at room temperature. Excluding oxygen redirects the same radical manifold toward productive C−H functionalization, enabling selective grafting of maleimide and maleic anhydride onto the PE backbone. Subsequent amine coupling of the anhydride moieties affords amide-functionalized PE architectures, demonstrating the synthetic versatility of the grafted handles. Future work will broaden the scope of grafting partners, probe structure−reactivity relationships in complex polyolefin blends, and evaluate translation to real-world plastic waste streams under process-relevant conditions.

■ ASSOCIATED CONTENT

Supporting Information

The Supporting Information is available free of charge at https://pubs.acs.org/doi/10.1021/acsmacrolett.6c00309.

Experimental protocols, ^{1}H NMR spectra, SEC traces, and mass spectra (Figures S1−S43, Schemes S1−S12, Tables S1−S7) (PDF)

■ AUTHOR INFORMATION

Corresponding Authors

Eva Harth − *Center of Excellence in Polymer Chemistry (CEPC), Department of Chemistry, University of Houston, Houston, Texas 77204, United States;* orcid.org/0000-0001-5553-0365; Email: harth@uh.edu

Cyrille Boyer − *School of Chemical Engineering, UNSW Sydney, Sydney, New South Wales 2052, Australia;* orcid.org/0000-0002-4564-4702; Email: cboyer@unsw.edu.au

Authors

Manish Kumar − *School of Chemical Engineering, UNSW Sydney, Sydney, New South Wales 2052, Australia;* orcid.org/0009-0009-6439-150X

Zhisheng Lin − *School of Chemical Engineering, UNSW Sydney, Sydney, New South Wales 2052, Australia*

Stephen Don Sarkar − *Center of Excellence in Polymer Chemistry (CEPC), Department of Chemistry, University of Houston, Houston, Texas 77204, United States;* orcid.org/0000-0001-8541-3629

Complete contact information is available at: https://pubs.acs.org/10.1021/acsmacrolett.6c00309

Notes

The authors declare no competing financial interest.

■ ACKNOWLEDGMENTS

The authors thank the UNSW MWAC facility for providing NMR access and the Bioanalytical Mass Spectrometry Facility (BMSF) for their assistance. CB acknowledges his Australian Laureate Fellowship (FL220100016) from the Australian Research Council. S.D.S. and E.H. thank the Robert A. Welch Foundation, USA, for the generous support of this research (H-E-0041, E-2066- 202110327, and E-2066-20240404) through the Center of Excellence in Polymer Chemistry and also gratefully acknowledge the National Science Foundation, USA, for supporting parts of this work (CHEM-2108576 and 2404432).

REFERENCES

(1) Policy Scenarios for Eliminating Plastic Pollution by 2040, 2024. https://www.oecd.org/en/publications/policy-scenarios-for-eliminating-plastic-pollution-by-2040_76400890-en.html (accessed 2026 April).

(2) Plastics the Fast Facts 2025, 2025. https://plasticseurope.org/knowledge-hub/plastics-the-fast-facts-2025/ (accessed 2026 April).

(3) Jeremic, D. Polyethylene. *Ullmann's Encyclopedia of Industrial Chemistry*; Wiley, 2014; pp 1−42.

(4) Sarkar, S. D.; Harth, E. Access to Polyethylene-Polyester Block Copolymers in Continuous Flow through Single-Step Chain-End-Functionalized Polyethylene. *JACS Au* **2026**, *6* (2), 821−829.

(5) Arslan, M.; Liu, Y. S.; Deydier, E.; Poli, R.; Harth, E. Leveraging Earth-Abundant Nickel for Orthogonal Polymerizations: Synthesizing Polar Polyolefin Block Copolymers. *J. Am. Chem. Soc.* **2025**, *147* (45), 41678−41690.

(6) Kim, K.; Strong, J.; Sarkar, S. D.; Nguyen, D.; Dau, H.; Al-Aman, D. A. A.; Dadashi-Silab, S.; Harth, E.; Matyjaszewski, K. Polyethylene-poly(methyl acrylate) Block Copolymers from PACE-SARA ATRP: Utilizing Polyolefin Active Ester Exchange-Based Macroinitiators in Atom Transfer Radical Polymerization. *Macromolecules* **2025**, *58* (3), 1337−1348.

(7) Zhao, C.; Harth, E. Polar polyethylene block copolymer synthesis via organometallic-mediated radical polymerization using Co(Salen) complexes. *Eur. Polym. J.* **2024**, *220*. 113460.

(8) Sarkar, S. D.; Dau, H.; Harth, E. Synthesis of polyethylene-polyacrylate block copolymers in continuous flow. *Chem.* **2024**, *10* (9), 2872−2886.

(9) Dau, H.; Tsogtgerel, E.; Matyjaszewski, K.; Harth, E. One-For-All Polyolefin Functionalization: Active Ester as Gateway to Combine Insertion Polymerization with ROP, NMP, and RAFT. *Angew. Chem., Int. Ed. Engl.* **2022**, *61* (33), No. e202205931.

(10) Geyer, R.; Jambeck, J. R.; Law, K. L. Production, use, and fate of all plastics ever made. *Sci. Adv.* **2017**, *3* (7), No. e1700782.

(11) MacLeod, M.; Arp, H. P. H.; Tekman, M. B.; Jahnke, A. The global threat from plastic pollution. *Science* **2021**, *373* (6550), 61−65.

(12) Ostle, C.; Thompson, R. C.; Broughton, D.; Gregory, L.; Wootton, M.; Johns, D. G. The rise in ocean plastics evidenced from a 60-year time series. *Nat. Commun.* **2019**, *10* (1), 1622.

(13) Singh, N.; Walker, T. R. Plastic recycling: A panacea or environmental pollution problem. *Npj Mater. Sustain* **2024**, *2* (1), 17.

(14) Wei, F.; Wei, E.; Chen, Y.; Li, J.; Tan, Q. Recycle or Not? An Exploration of Microplastic Generation During Plastic Processing via a Local Case Study. *Environ. Sci. Technol.* **2024**, *58* (48), 21374−21383.

(15) Su, J.; Li, T.; Xie, W.; Wang, C.; Yin, L.; Yan, T.; Wang, K. Emerging Technologies for Waste Plastic Treatment. *ACS Sustainable Chem. Eng.* **2023**, *11* (22), 8176−8192.

(16) Patel, A. D.; Schyns, Z. O. G.; Franklin, T. W.; Shaver, M. P. Defining quality by quantifying degradation in the mechanical recycling of polyethylene. *Nat. Commun.* **2024**, *15* (1), 8733.

(17) Koelmans, A. A.; Redondo-Hasselerharm, P. E.; Nor, N. H. M.; de Ruijter, V. N.; Mintenig, S. M.; Kooi, M. Risk assessment of microplastic particles. *Nat. Rev. Mater.* **2022**, *7* (2), 138−152.

(18) Coates, G. W.; Getzler, Y. D. Y. L. Chemical recycling to monomer for an ideal, circular polymer economy. *Nat. Rev. Mater.* **2020**, *5* (7), 501−516.

(19) Yan, J.; Li, G.; Lei, Z.; Yuan, X.; Li, J.; Wang, X.; Wang, B.; Tian, F.; Hu, T.; Huang, L.; et al. Upcycling polyolefins to methane-free liquid fuel by a Ru(1)-ZrO(2) catalyst. *Nat. Commun.* **2025**, *16* (1), 2800.

(20) Wimberger, L.; Ng, G.; Boyer, C. Light-driven polymer recycling to monomers and small molecules. *Nat. Commun.* **2024**, *15* (1), 2510.

(21) Jehanno, C.; Alty, J. W.; Roosen, M.; De Meester, S.; Dove, A. P.; Chen, E. Y.; Leibfarth, F. A.; Sardon, H. Critical advances and future opportunities in upcycling commodity polymers. *Nature* **2022**, *603* (7903), 803−814.

(22) Oh, S.; Stache, E. E. Chemical Upcycling of Commercial Polystyrene via Catalyst-Controlled Photooxidation. *J. Am. Chem. Soc.* **2022**, *144* (13), 5745−5749.

(23) Oh, S.; Stache, E. E. Mechanistic Insights Enable Divergent Product Selectivity in Catalyst-Controlled Photooxidative Degradation of Polystyrene. *ACS Catal.* **2023**, *13* (16), 10968−10975.

(24) Oh, S.; Jiang, H.; Kugelmass, L. H.; Stache, E. E. Recycling of Post-Consumer Waste Polystyrene Using Commercial Plastic Additives. *ACS Central Science* **2025**, *11* (1), 57−65.

(25) Jiang, H.; Medina, E. A.; Stache, E. E. Upcycling Poly(vinyl chloride) and Polystyrene Plastics Using Photothermal Conversion. *J. Am. Chem. Soc.* **2025**, *147* (3), 2822−2828.

(26) Flanders, M. J.; Gramlich, W. M. Reversible-addition fragmentation chain transfer (RAFT) mediated depolymerization of brush polymers. *Polym. Chem.* **2018**, *9* (17), 2328−2335.

(27) Raus, V.; Čadová, E.; Starovoytova, L.; Janata, M. ATRP of POSS Monomers Revisited: Toward High-Molecular Weight Methacrylate−POSS (Co)Polymers. *Macromolecules* **2014**, *47* (21), 7311−7320.

(28) Wang, H. S.; Truong, N. P.; Pei, Z.; Coote, M. L.; Anastasaki, A. Reversing RAFT Polymerization: Near-Quantitative Monomer Generation Via a Catalyst-Free Depolymerization Approach. *J. Am. Chem. Soc.* **2022**, *144* (10), 4678−4684.

(29) Kumar, M.; Michelas, M.; Boyer, C. Microwave-Assisted Depolymerization of Polymethacrylates. *ACS Macro Lett.* **2025**, *14* (7), 940−947.

(30) Young, J. B.; Hughes, R. W.; Tamura, A. M.; Bailey, L. S.; Stewart, K. A.; Sumerlin, B. S. Bulk depolymerization of poly(methyl methacrylate) via chain-end initiation for catalyst-free reversion to monomer. *Chem.* **2023**, *9* (9), 2669−2682.

(31) Martinez, M. R.; Schild, D.; De Luca Bossa, F.; Matyjaszewski, K. Depolymerization of Polymethacrylates by Iron ATRP. *Macromolecules* **2022**, *55* (23), 10590−10599.

(32) Young, J. B.; Bowman, J. I.; Eades, C. B.; Wong, A. J.; Sumerlin, B. S. Photoassisted Radical Depolymerization. *ACS Macro Lett.* **2022**, *11* (12), 1390−1395.

(33) Ng, G.; Prescott, S. W.; Postma, A.; Moad, G.; Hawker, C. J.; Anastasaki, A.; Boyer, C. Enhancing photothermal depolymerization with metalloporphyrin catalyst. *J. Polym. Sci.* **2024**, *62* (17), 3920−3928.

(34) Lohmann, V.; Poon, L. N.; Whitfield, R.; Matyjaszewski, K.; Mougel, V.; Anastasaki, A. Electrochemically Mediated Depolymerization of Polymers Synthesized by Atom Transfer Radical Polymerization. *J. Am. Chem. Soc.* **2026**, *148* (8), 8067−8072.

(35) Gilchrist, G. C.; Hughes, R. W.; Maity, T.; Gitter, S. R.; Izadi, N.; Marquez, J. D.; Young, J. B.; Evans, A. M.; Sumerlin, B. S. Electrochemically Initiated Depolymerization of Poly(Methyl Methacrylate). *J. Am. Chem. Soc.* **2026**, *148* (3), 3336−3342.

(36) Bi, T.; Chen, Y.; Lin, L.; Han, X.; Pan, Y.; Liu, C.; Cen, Z.; Luo, C.; Wen, W.; Zulfiqar, H.; et al. Closed-loop recycling of polyethylene to ethylene and propylene via a kinetic decoupling−recoupling strategy. *Nature Chemical Engineering* **2025**, *2* (10), 650−661.

(37) Otten, M.; Klein Gebbink, I.; Schara, P. J.; Tomovic, Z.; Lutz, M.; Bruijnincx, P. C. A.; Thevenon, A. Post-Polymerization Modification of Polyethylene through Photochemical Oximation and Consecutive Ketonization. *J. Am. Chem. Soc.* **2025**, *147* (26), 22827−22838.

(38) Lemmens, R.; Vercammen, J.; Van Belleghem, L.; De Vos, D. Upcycling polyethylene into closed-loop recyclable polymers through titanosilicate catalyzed C-H oxidation and in-chain heteroatom insertion. *Nat. Commun.* **2024**, *15* (1), 9188.

(39) Cui, S.; Lu, Z.; Lopez, J. C.; Kranzlein, M.; Kim, C. J.; Lin, S.; LaPointe, A. M.; Coates, G. W. Main-Chain Ketone Installation in Polyethylene Chains: A Metal-Free Strategy toward Photodegradable Plastics. *J. Am. Chem. Soc.* **2025**, *147* (41), 37204−37210.

(40) Arroyave, A.; Cui, S.; Lopez, J. C.; Kocen, A. L.; LaPointe, A. M.; Delferro, M.; Coates, G. W. Catalytic Chemical Recycling of Post-Consumer Polyethylene. *J. Am. Chem. Soc.* **2022**, *144* (51), 23280−23285.

https://doi.org/10.1021/acsmacrolett.6c00309
ACS Macro Lett. XXXX, XXX, XXX−XXX

(41) Capaldo, L.; Ravelli, D.; Fagnoni, M. Direct Photocatalyzed Hydrogen Atom Transfer (HAT) for Aliphatic C-H Bonds Elaboration. *Chem. Rev.* **2022**, *122* (2), 1875−1924.
(42) Williamson, J. B.; Lewis, S. E.; Johnson, R. R., 3rd; Manning, I. M.; Leibfarth, F. A. C-H Functionalization of Commodity Polymers. *Angew. Chem., Int. Ed. Engl.* **2019**, *58* (26), 8654−8668.
(43) Fazekas, T. J.; Alty, J. W.; Neidhart, E. K.; Miller, A. S.; Leibfarth, F. A.; Alexanian, E. J. Diversification of aliphatic C−H bonds in small molecules and polyolefins through radical chain transfer. *Science* **2022**, *375* (6580), 545−550.
(44) Oh, S.; Stache, E. E. Recent advances in oxidative degradation of plastics. *Chem. Soc. Rev.* **2024**, *53* (14), 7309−7327.
(45) Stache, E. E.; Kottisch, V.; Fors, B. P. Photocontrolled Radical Polymerization from Hydridic C-H Bonds. *J. Am. Chem. Soc.* **2020**, *142* (10), 4581−4585.
(46) Neidhart, E. K.; Hua, M.; Peng, Z.; Kearney, L. T.; Bhat, V.; Vashahi, F.; Alexanian, E. J.; Sheiko, S. S.; Wang, C.; Helms, B. A.; et al. C-H Functionalization of Polyolefins to Access Reprocessable Polyolefin Thermosets. *J. Am. Chem. Soc.* **2023**, *145* (50), 27450−27458.
(47) Kumar, M.; Michelas, M.; Boyer, C. Polymer Chain Modification via HAT Chemistry and Its Application in Graft Copolymer Synthesis. *ACS Macro Lett.* **2025**, *14* (4), 396−404.
(48) Kranzlein, M.; Cui, S.; Hu, J.; LaPointe, A. M.; Fors, B. P.; Coates, G. W. One-Step Radical-Induced Synthesis of Graft Copolymers for Effective Compatibilization of Polyethylene and Polypropylene. *J. Am. Chem. Soc.* **2025**, *147* (22), 19052−19060.
(49) Hsu, J. H.; Ball, T. E.; Oh, S.; Stache, E. E.; Fors, B. P. Selective Electrocatalytic Degradation of Ether-Containing Polymers. *Angew. Chem., Int. Ed. Engl.* **2024**, *63* (3), No. e202316578.
(50) Barber, V. J.; Borden, M. A.; Alty, J. W.; Tran, L. D.; Koerner, H.; Baldwin, L. A.; Alexanian, E. J.; Leibfarth, F. A. Modifying Poly(caprolactone) Degradation through C-H Functionalization. *Macromolecules* **2023**, *56* (10), 3679−3686.
(51) Wang, H. S.; Agrachev, M.; Kim, H.; Truong, N. P.; Choi, T. L.; Jeschke, G.; Anastasaki, A. Visible light−triggered depolymerization of commercial polymethacrylates. *Science* **2025**, *387* (6736), 874−880.
(52) Michelas, M.; Kumar, M.; Lin, Z.; Boyer, C. In Situ Modification Assisted by HAT Chemistry for the Main Chain Initiated Depolymerization of Polymethacrylates. *ACS Macro Lett.* **2025**, *14*, 822−829.
(53) Ringuette, A. E.; Aktas Eken, G.; Garnenez, A. B.; Palmieri, A. I.; Ober, C. K.; Coates, G. W.; Fors, B. P. Direct Functionalization of Polyethylene Surfaces with High-Density Polymer Brushes. *J. Am. Chem. Soc.* **2024**, *146* (30), 20563−20568.
(54) Tran, Q. H.; Neidhart, E. K.; Sheiko, S. S.; Bras, W.; Leibfarth, F. A. Polyolefin Ionomer Synthesis Enabled by C−H Thioheteroarylation. *Macromolecules* **2023**, *56* (21), 8920−8927.
(55) Zhang, M.; Kranzlein, M.; Cui, S.; LaPointe, A. M.; Coates, G. W. C-H Insertion Functionalization of Polyolefins for Versatile Polyolefin-Polyester Compatibilization. *J. Am. Chem. Soc.* **2026**, *148* (4), 4599−4604.
(56) Plummer, C. M.; Zhou, H.; Li, S.; Zhong, H.; Sun, Z.; Bariashir, C.; Sun, W.-H.; Huang, H.; Liu, L.; Chen, Y. A direct functionalization of polyolefins for blend compatibilization by an insertion of 1,1-bis(phenylsulfonyl)ethylene (BPSE). *Polym. Chem.* **2019**, *10* (24), 3325−3333.
(57) Li, C.; Kong, X. Y.; Lyu, M.; Tay, X. T.; Đokić, M.; Chin, K. F.; Yang, C. T.; Lee, E. K. X.; Zhang, J.; Tham, C. Y.; et al. Upcycling of non-biodegradable plastics by base metal photocatalysis. *Chem.* **2023**, *9* (9), 2683−2700.
(58) Zhang, S.; Wang, J.; Su, D.; Xiao, X. Facile visible-light upcycling of diverse waste plastics using a single organocatalyst with minimal loadings. *Nat. Commun.* **2025**, *16* (1), 4188.
(59) Nikitas, N. F.; Skolia, E.; Gkizis, P. L.; Triandafillidi, I.; Kokotos, C. G. Photochemical aerobic upcycling of polystyrene plastics to commodity chemicals using anthraquinone as the photocatalyst. *Green Chem.* **2023**, *25* (12), 4750−4759.
(60) Shaibu, A.; Tijani, J. O.; Abdulkareem, A. S.; Mustapha, S. I.; Mustapha, S.; Baba, I. A. Photocatalytic degradation of polyethylene films using green-synthesized ZnO and Fe(3)O(4) nanoparticles from Acacia nilotica. *Sci. Rep* **2026**, DOI: 10.1038/s41598-026-43013-w.
(61) Zhang, Q.; Wei, X.; Shen, C.; Ye, P.; An, W.; Liu, X.; Xu, S.; Wang, Y.-Z. Solvent-Regulated Tandem Oxidative Degradation of Polyethylene to Multifunctional Chemicals. *ACS Sustainable Chem. Eng.* **2024**, *12* (15), 5788−5798.
(62) Choi, S.; Jang, S.; Do, G.; Lee, P. C.; Choi, D. Optimizing maleic anhydride content to enhance mechanical performance and thermal stability of recycled polyolefin blends. *Sci. Rep* **2026**, *16* (1), 1234.
(63) Graziano, A.; Titton Dias, O. A.; Sena Maia, B.; Li, J. Enhancing the mechanical, morphological, and rheological behavior of polyethylene/polypropylene blends with maleic anhydride-grafted polyethylene. *Polym. Eng. Sci.* **2021**, *61* (10), 2487−2495.
(64) Smith, M. P.; Klumperman, B. Maleic Anhydride and Its Derivatives: A Brief Review of Reactivity and Properties in Radical (Co)Polymerizations. *Macromol. Rapid Commun.* **2025**, *46* (24), No. e00551.
(65) Yang, L.; Zhang, F.; Endo, T.; Hirotsu, T. Microstructure of Maleic Anhydride Grafted Polyethylene by High-Resolution Solution-State NMR and FTIR Spectroscopy. *Macromolecules* **2003**, *36* (13), 4709−4718.

https://doi.org/10.1021/acsmacrolett.6c00309
ACS Macro Lett. XXXX, XXX, XXX−XXX